crystals

MDPI

Article

# Effect of Nitrogen Impurities on the Raman Line Width in Diamond, Revisited

**Nikolay V. Surovtsev [1,2] and Igor N. Kupriyanov [3,*]**

[1] Institute of Automation and Electrometry, Siberian Branch of the Russian Academy of Sciences, Koptyug ave., 1, 630090 Novosibirsk, Russia; lab04@iae.nsk.su
[2] Department of Physics, Novosibirsk State University, 630090 Novosibirsk, Russia
[3] Sobolev Institute of Geology and Mineralogy, Siberian Branch of the Russian Academy of Sciences, Koptyug ave., 3, 630090 Novosibirsk, Russia
* Correspondence: spectra@igm.nsc.ru; Tel.: +7-383-330-7501

Academic Editor: Yuri N. Palyanov
Received: 30 June 2017; Accepted: 28 July 2017; Published: 31 July 2017

**Abstract:** The results of a high-resolution Raman scattering study of a diamond crystal with a high content of single substitutional nitrogen impurities (550 ppm) in the temperature range from 50 to 673 K are presented and compared with the data for defect-free diamond. It is established that the increase of the nitrogen concentration in diamond leads to the temperature-independent increase of the Raman line width. Analysis of the experimental data allows us to conclude that this broadening should be attributed to the defect-induced shortening of the Raman phonon lifetime. We believe that this mechanism is responsible for the increase of the Raman line width caused by most point-like defects in diamond. No pronounced effects of the nitrogen defects on the Raman line position and phonon anharmonicity are observed.

**Keywords:** diamond; Raman scattering; Raman linewidth; nitrogen defects

## 1. Introduction

Raman scattering spectroscopy has proven to be an effective and powerful technique to characterize diamond and diamond-related materials synthesized under different conditions [1–10]. The first-order Raman scattering spectrum of diamond is one of the simplest of its kind and consists of a single narrow line at around 1332 $cm^{-1}$. Various structural imperfections present in the diamond crystal affect its Raman spectrum. The occurrence of internal strains leads to Raman line shift; fluctuations of interatomic interaction and shortening of the phonon lifetime cause Raman line broadening; the presence of defects and impurities gives rise to new lines in the spectrum. Transformation to other phases (e.g., graphite-like) also would lead to the change of the Raman spectrum. Thus, the study of Raman spectra with an emphasis on the line position and width can help in the characterization of diamonds and diamond-related materials. This message has been exploited in a prodigious number of works [11–20].

An important prerequisite for the correct interpretation of the changes in the Raman line position and width is a clear understanding of the mechanisms responsible for these changes. Despite the long prehistory of experimental and model descriptions of the Raman line in diamond, it is only recently that the ultimate experimental information has been obtained for the temperature dependence of the Raman line width in defect-free diamond [21]. It is found that, for nearly perfect diamond crystals containing negligible amounts of lattice defects and impurities, the Raman line width is described exclusively by three-phonon and four-phonon anharmonic processes. Since, in most cases, Raman spectroscopy characterization of diamond materials is performed at room temperature, the question arises of how the defect-induced contribution to the Raman line width should be described.

This question pursues whether it is due to the changes of anharmonicity, or local fluctuations of the optical phonon frequency, or the relaxation of the Raman wavevector selection rule caused by phonon confinement, or the change of phonon wavefunction as solution of the dynamic problem, or something else.

It has previously been determined that nitrogen centers in diamond lead to the increase of the Raman line width proportional to the nitrogen concentration [22,23]. However, both these works were undertaken at room temperature and it is not clear which mechanism of the Raman line broadening is responsible for this outcome. In the present work, we demonstrate that the study of the temperature dependence of the Raman line recorded with a high spectral resolution can resolve this problem.

## 2. Results

Due to the anharmonic effects, the Raman line width of diamond decreases with decreasing temperature. Therefore, the defect-induced broadening is better manifested in the spectra measured at low temperatures. Figure 1 shows the Raman line contours of the diamond sample with high nitrogen concentration (550 ppm) and of the defect-free diamond [21], recorded at 50 K, which was the lowest temperature in our experiments. As it can be seen, the presence of substitutional nitrogen defects leads to a significant broadening of the Raman line. At the same time, the position of the Raman line is barely, if at all, changed. The broadening induced by nitrogen defects is slightly asymmetric, but the asymmetry is low. An asymmetry factor defined as the difference between the spectral position of the maximum and the mean position at the half-maximum level is 0.07 $cm^{-1}$ in the case of the nitrogen-containing diamond, while the width difference between the spectra of the defect-free diamond and of the diamond with nitrogen at the half-maximum level is 0.83 $cm^{-1}$. Thus, with this low asymmetry, we can consider the main component of the defect-induced broadening as symmetric and make use of symmetric contours for the description of the experimental Raman lines.

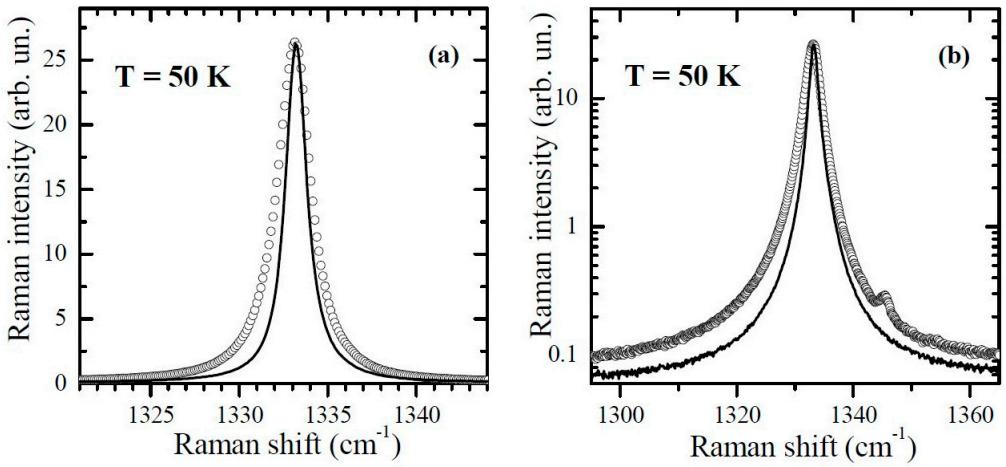


**Figure 1.** Raman line of the nitrogen-containing diamond (circles) and of the defect-free diamond (line) at T = 50 K: (**a**) linear scale for the intensity; (**b**) logarithmic scale for the intensity.

Another interesting feature of the Raman spectrum of the nitrogen-containing diamond is the occurrence of an additional weak peak located at 1345.5 $cm^{-1}$ at T = 50 K. This peak is attributed to the well-known localized vibrational mode originating at substitutional nitrogen defects. This is a characteristic feature of the IR absorption spectrum of single substitutional nitrogen defects in diamond appearing at 1344 $cm^{-1}$ at room temperature. To the best of our knowledge, this is the first time that this nitrogen-related localized mode is detected by Raman scattering. This finding opens certain prospects for the use of Raman scattering for probing the nitrogen content of micro- and nano-diamonds, for which conventional IR absorption spectroscopy cannot easily be applied. For the

spectrum shown in Figure 1, it is found that the relative intensity of the 1345.5 $cm^{-1}$ local mode peak to the diamond Raman line is about (2.5–3.0) $\times$ $10^{-3}$.

As we have demonstrated previously, the Raman line of diamond crystals with a negligible amount of defects can be well described by the Voigt contour, where the Gaussian component reflects the spectral resolution of the experimental setup (0.3 $cm^{-1}$ in our experiments) and the Lorentzian component reflects the broadening caused by anharmonicity [21]. The results of the Voigt contour fitting applied to the Raman spectrum of the nitrogen-containing diamond are shown in Figure 2. It is found that fits with both the fixed Gaussian component (width set to 0.3 $cm^{-1}$) and with the free parameter describe the experimental line contour with good quality. However, if we suppose that the defect-induced broadening has a Gaussian-like contribution and fix the Lorentzian width, setting it to a value found for the defect-free diamond, then the quality of the fit notably decreases. Therefore, we may conclude that the substitutional nitrogen defects causes the Lorentzian-like broadening of the Raman line of diamond.

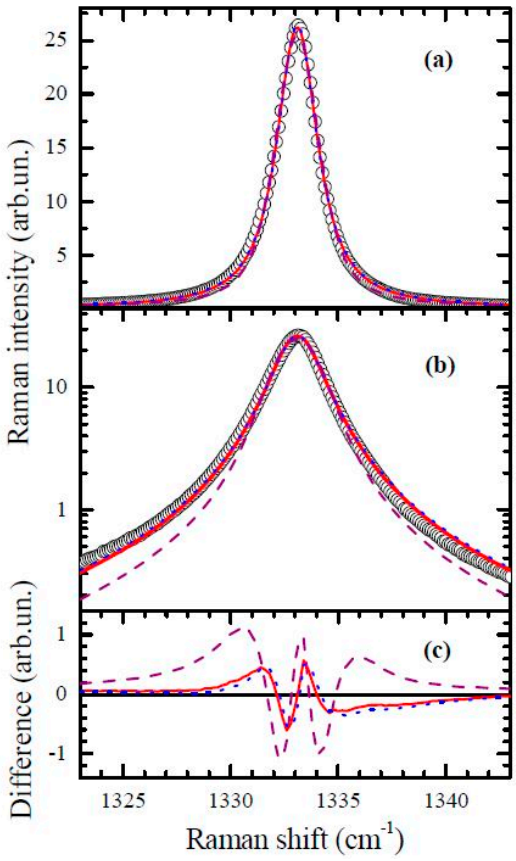


**Figure 2.** Raman line of the diamond with nitrogen impurities at T = 50 K (circles) and fitting curves, represented in (**a**) linear and (**b**) logarithmic scale for the intensity. The solid line is the Voight contour fit without restrictions for the fitting parameters; the dotted line is the Voight contour fit with the Gaussian width fixed to the instrumental resolution; the dashed line is the Voight contour fit with the Lorentzian width fixed to that of the Raman line of the defect-free diamond. (**c**) Differences between the experimental data and the fitting curves, employing the same designations as in (**a**,**b**).

Figure 3 shows the temperature dependence of the Raman line position and width extracted from the Voigt fit of the Raman spectra of the nitrogen-containing diamond and defect-free diamond. It can be seen that the spectral positions of the Raman line are very close for these two diamonds, and that they follow the same temperature dependence. The model description of the Raman line shift with temperature, being still a matter of research [24,25], lies beyond the scope of the present work and is

not addressed here. The Lorentzian line width of the diamonds with and without nitrogen is different, but the difference is temperature independent. Three-phonon and four-phonon anharmonic processes contribute to the Lorentzian line width of the defect-free diamond, which is described by [26]:

$$\Gamma_L(T) = A(2n(\omega_0/2, T) + 1) + B(3n^2(\omega_0/3, T) + 3n(\omega_0/3, T) + 1), \quad (1)$$

where n(ω,T) is the Bose-Einstein distribution and A and B are the fitting parameters, which for the defect-free diamond are equal to 1.15 $cm^{-1}$ and 0.2 $cm^{-1}$, respectively [21]. The description by Equation (1) is shown in Figure 3 for the data of the defect-free diamond. We find that the same function curve, except shifted upward by 0.87 $cm^{-1}$, also describes the experimental Lorentzian line width of the nitrogen-containing diamond very well. Thus, it follows that substitutional nitrogen defects in concentrations at the level of 550 ppm do not produce noticeable changes of the lattice anharmonicity, and the defect-induced broadening of the Raman line is temperature-independent.

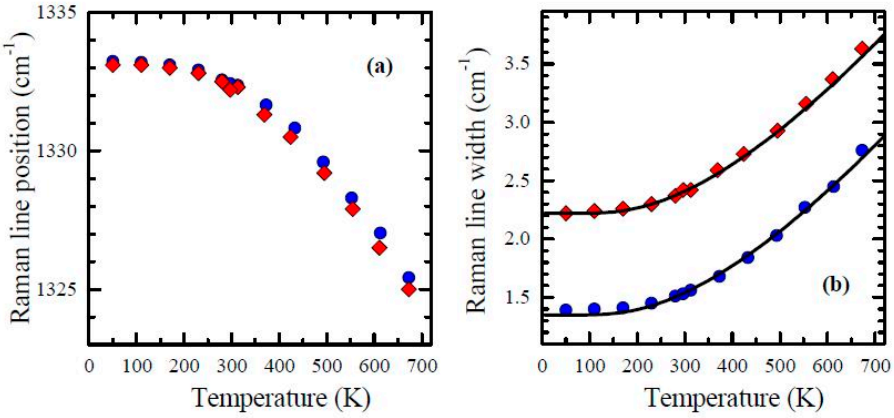


**Figure 3.** Temperature dependences of the Raman line parameters of the nitrogen-containing diamond (diamonds) and defect-free diamond (circles): (**a**) line position; (**b**) Lorentzian line width. The lines depict fits by Equation (1) (see text for details).

## 3. Discussion

The results of this study reveal that the single substitutional nitrogen defects does not change the anharmonicity of the optical phonon in diamond. In principle, one could suppose that the quasi-localized vibrational modes induced in diamond by nitrogen defects, whose local density of states extends below 500 $cm^{-1}$ [27], may participate in the anharmonic decay of the Raman phonon. Furthermore, due to symmetry breaking, the decay of the Raman phonon into defect-induced quasi-localized modes could occur with the violation of the wavevector conservation law. Should this hold true, the occurrence of the additional channels for the anharmonic decay of the Raman phonon would modify the temperature dependence of the Raman line width. This, however, as demonstrated by our results, is not the case. With the high precision, the same anharmonic decay process, with the same parameters, describe the temperature-dependent part the Raman line width of both defect-free and nitrogen-containing diamonds. As a consequence, the defect-induced contribution to the Raman line width of a diamond crystal determined from room temperature measurements can be considered representative for the temperature-independent Raman line broadening caused by the defects, at least if the considered defect concentration is of the order of 500 ppm.

The results presented in Figures 1 and 2 demonstrate that the nitrogen concentration leads to an additional Lorentz-like broadening of the Raman line. In the case when the additional broadening would be caused by a distribution of the phonon frequency a Gaussian-like broadening is expected. Thus, the distributions of nitrogen and of defect-induce lattice distortions are uniform at the scale of the coherence volume of the optical phonon taking part in Raman scattering.

Most of the previous models dealing with the defect-induced changes of the Raman line width in diamond or similar crystals consider the relaxation of the wavevector selection rules caused by defects [28,29] as the main mechanism of the effect of the defects on the Raman spectrum. It can be described by relatively simple estimations involving the uncertainty principle [30] or by solving the equation for the phonon Green's function [31]; however, their outcomes are qualitatively similar—a shift and an accompanied broadening of the Raman line are expected. In this case, the broadened contour of defective crystals usually does not exceed the tail of the Raman contour of a defect-free crystal at either the high or low frequency side (see, for examples, figures in References [28,31]). From our results, it follows that this does not hold for the nitrogen-containing diamond, where defect-induced broadening for both sides of the Raman line is observed and the defect-induced shift of the Raman line is negligible. Furthermore, it should be noted that, as it is demonstrated by Richter et al. [30], the relaxation of the wavevector conservation law in the case of phonon confinement modifies the temperature dependence of the Raman line width. This, again, as demonstrated by our results, is not the case for nitrogen defects in diamond. While the phonon confinement model cannot describe the observed Raman line broadening correctly, we admit that the observed slight asymmetry of the Raman contour (Figure 1) could be attributed to a contribution of the phonon states in the vicinity of the Brillouin-zone center (Γ point) due to the partial breakdown of the wavevector selection rules.

A mechanism of the defect-induced shortening of the optical phonon lifetime is apparently more appropriate for the case of substitutional nitrogen defects in diamond. However, it is necessary to point out that the zone-center optical phonon has nearly zero group velocity and should be considered as not a propagating, but as an effectively standing wave. This means that the idea of the phonon mean free path evoked to describe the defect-induced scattering of acoustic phonons cannot be easily applied in the present case. To overcome this controversy, we note that the true harmonic solutions of the vibrational problem for a defective crystal are not plane waves, so the optical phonon created by the Raman process is not a vibrational eigenmode of the defective crystal. The standing wave of the optical phonon created by the Raman process undergoes elastic scattering by defects, which act as Rayleigh scatters. This leads to the attenuation of the Raman phonon, shortening its lifetime. The attenuation should be proportional to the defect concentration and result in an additional Lorentzian-like broadening, which is independent of temperature. No sharp dependence of the Raman line position on impurity concentration is expected in this case. The results of this work and the previous observations [22,23] agree well with the proposed mechanism of the defect-induced effects on the Raman line in diamonds.

In an attempt to provide a quantitative description accrued from the above model, we note that the defect-induced increase of the dissipation factor of the Raman phonon is proportional to the fractional concentration of defects, $c_d$, and for the defect-induced broadening, $\gamma$, one can write:

$$\gamma = F\omega_0 c_d, \quad (2)$$

where $\omega_0$ is the phonon frequency (for diamond $\omega_0 = 1332$ cm$^{-1}$) and F is a dimensionless constant. For the rough estimation, the magnitude of F is an order of unity. With the nitrogen concentration of 550 ppm and F = 1, one obtains the estimation of $\gamma \approx 0.7$ cm$^{-1}$, which is remarkably close to the experimentally established value of 0.87 cm$^{-1}$. Such closeness is rather fortuitous, since F = 1 has the sense of estimation by an order of magnitude. Nevertheless, we see that the estimation by Equation (2) provides the correct order of magnitude, and it is convenient to characterize different impurities by their value of F.

In accord with previous observations [22,23], our results show that single substitutional nitrogen defects in diamond cause significant Raman line broadening, but produce very subtle effects on the Raman line position. Even for a diamond crystal with a relatively high nitrogen content (550 ppm), the shift of the Raman frequency cannot be determined with confidence as being within the accuracy of the line-center measurements (about 0.3 cm$^{-1}$ absolute value in our experiment). On the other hand, it is well known that the presence of nitrogen impurities in diamond results in an increase in the

lattice parameter [32]. This lattice dilatation should in turn manifest in the change of the Raman line position, representing the lower limit of the Raman frequency shift caused by nitrogen defects. It is therefore of interest to estimate the magnitude of this effect. Lang et al. [32] found that the dilation of the diamond lattice by single substitutional nitrogen can be described by $\Delta a/a = 0.14 \times c(N)$, where c(N) is the fractional atomic concentration of substitutional nitrogen. For the diamond sample used in the present work, c(N) is equal to $5.5 \times 10^{-4}$ and consequently the produced lattice dilatation $\Delta a/a$ is equal to $7.7 \times 10^{-5}$. For small lattice parameter changes, we can assume the equivalence of tensile and compressive stresses and use the bulk modulus of diamond B = 442 $GPa^{-1}$ and the hydrostatic pressure coefficient of the Raman line of 3.2 $cm^{-1}$/GPa [33]. Our calculations show that, for a diamond crystal containing 550 ppm of substitutional nitrogen, a Raman frequency shift of 0.33 $cm^{-1}$ can be expected. This value is in reasonable agreement with our observations, so that we may speculate that the main effect of nitrogen impurities on the diamond Raman frequency is through the change of the diamond lattice parameters. Obviously, further investigations employing diamonds with even higher nitrogen content are necessary to verify this hypothesis.

## 4. Materials and Methods

Synthetic diamond crystal were grown by the temperature gradient growth method using a high-pressure multi-anvil apparatus of the split-sphere type [34]. A $Co_{0.7}Fe_{0.3}$ alloy was used as the solvent-catalyst. To produce diamond crystals with high nitrogen concentrations, nitrogen-containing compounds, $CaCN_2$ and $Fe_3N$, were added to the charge. The growth experiments were typically run at 5.5 GPa and 1400 °C for 65 h. For the purpose of the present study, a high-quality octahedral diamond crystal weighting about 2 ct and showing no metallic inclusions was selected. Using laser cutting and mechanical chipping, a plate was cleaved from the outer part of the crystal and then polished from two sides. The produced diamond plate, consisting of a single (111) growth sector, had a thickness of approximately 1 mm and linear size of 4–5 mm. The concentration of nitrogen impurities was determined using infrared (IR) absorption spectroscopy. The spectra were acquired from different locations over the sample using a Bruker Vertex 70 FTIR spectrometer fitted with a Hyperion 2000 microscope (Bruker Optics, Ettlingen, Germany). A representative IR spectrum of the diamond sample is shown in Figure 4. The concentration of nitrogen impurities in the form of single substitutional nitrogen atoms (C-centers) and nitrogen pairs (A-centers) was determined by decomposing the defect-induced absorption into the C and A components and using known conversion factors [35]. It was found that the concentration of the C form nitrogen in the sample varied within 540–560 ppm, and that of the A form nitrogen varied within 20–30 ppm. Taking into account the results of our previous study [23], we can neglect the effect of the small concentration of the A-centers, and take the average value of 550 ppm as the representative concentration of the single substitutional nitrogen defects in the studied diamond sample.

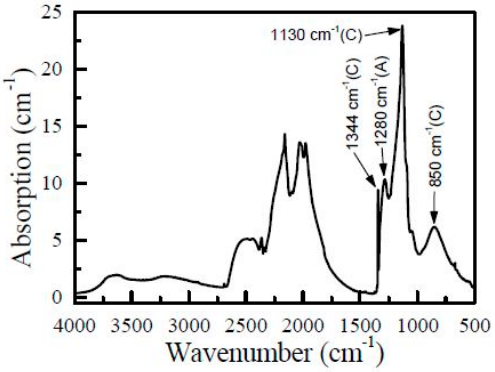


**Figure 4.** A representative infrared absorption spectrum of the diamond sample used in the study. The main absorption features related to the C- and A-centers are indicated.

The techniques and conditions employed for the Raman scattering experiment, as well as the spectral data processing, were the same as those used in our previous work [21]. Shortly, the Raman scattering measurements were carried out with excitation by the 514.5-nm line of an Ar-ion laser with a power of 100 mW. The spectra were recorded in a back-scattering geometry without polarization selection. An Acton TriVista 777 (Princeton Instruments, Acton, Santa Clara, CA, USA) triple spectrometer operated in the additive mode was used with 1800 groove/mm gratings. This configuration provides the pixel resolution of 0.1 $cm^{-1}$. The entrance slit was set to 30 microns. The instrumental spectral resolution was determined by experimental spectra of emission lines of a neon-discharge lamp, and found to be described by a Gaussian contour with a width of 0.3 $cm^{-1}$. The diamond sample was mounted in an optical closed-cycle cryostat or to a furnace for measurements at different temperatures. A temperature range from 50 to 700 K was covered in the Raman experiment.

## 5. Conclusions

From the results of the present study, the following main conclusions can be drawn: (1) The increase of the nitrogen concentration in diamond leads to additional Lorentz-like broadening of the Raman line; (2) This line width increase is independent of temperature and should be attributed to the defect-induced shortening of the Raman phonon lifetime. No pronounced effects of the nitrogen concentration on the Raman line position or anharmonicity are found. The present results establish that the increase of the Raman line width in diamonds containing point defects observed at room temperature relates to the decrease in the Raman phonon lifetime due to elastic scattering by defects.

**Acknowledgments:** We thank E.V. Podivilov for useful discussion and for attraction our attention to Equation (2). This work was supported by the Russian Science Foundation under Grant No. 14-27-00054. A part of the experiments was performed at the multiple-access center "High-resolution spectroscopy of gases and condensed matters" at IA&E SBRAS (Novosibirsk, Russia).

**Author Contributions:** The authors contributed equally to this work.

**Conflicts of Interest:** The authors declare no conflict of interest. The founding sponsors had no role in the design of the study; in the collection, analyses, or interpretation of data; in the writing of the manuscript, and in the decision to publish the results.

## References

1. Prawer, S.; Nemanich, R.J. Raman spectroscopy of diamond and doped diamond. *Philos. Trans. R. Soc. Lond. A* **2004**, *362*, 2537–2565. [CrossRef] [PubMed]
2. Ferrari, A.C.; Robertson, J. Raman spectroscopy of amorphous, nanostructured, diamond-like carbon, and nanodiamond. *Philos. Trans. R. Soc. Lond. A* **2004**, *362*, 2477–2512. [CrossRef] [PubMed]
3. Nakashima, S.; Harima, H. Raman investigation of SiC polytypes. *Phys. Status Solidi A* **1997**, *162*, 39–64. [CrossRef]
4. Bergman, L.; Nemanich, R.J. Raman and photoluminescence analysis of stress state and impurity distribution in diamond thin films. *J. Appl. Phys.* **1995**, *78*, 6709–6719. [CrossRef]
5. Blank, V.D.; Denisov, V.N.; Kirichenko, A.N.; Kuznetsov, M.S.; Mavrin, B.N.; Nosukhin, S.A.; Terentiev, S.A. Raman scattering by defect-induced excitations in boron-doped diamond single crystals. *Diam. Relat. Mater.* **2008**, *17*, 1840–1843. [CrossRef]
6. Gouadec, G.; Colomban, P. Raman spectroscopy of nanomaterials: How spectra relate to disorder, particle size and mechanical properties. *Prog. Cryst. Growth Charact. Mater.* **2007**, *53*, 1–56. [CrossRef]
7. Yap, C.M.; Tarun, A.; Xiao, S.; Misra, D.S. MPCVD growth of $^{13}C$-enriched diamond single crystals with nitrogen addition. *Diam. Relat. Mater.* **2016**, *63*, 2–11. [CrossRef]
8. Wu, G.; Chen, M.H.; Liao, J. The influence of recess depth and crystallographic orientation of seed sides on homoepitaxial growth of CVD single crystal diamonds. *Diam. Relat. Mater.* **2016**, *65*, 144–151. [CrossRef]
9. Prieske, M.; Vollertsen, F. In situ incorporation of silicon into a CVD diamond layer deposited under atmospheric conditions. *Diam. Relat. Mater.* **2016**, *65*, 47–52. [CrossRef]

10. Van Beveren, L.H.W.; Liu, R.; Bowers, H.; Ganesan, K.; Johnson, B.C.; McCallum, J.C.; Prawer, S. Optical and electronic properties of sub-surface conducting layers in diamond created by MeV B-implantation at elevated temperatures. *J. Appl. Phys.* **2016**, *119*, 223902. [CrossRef]
11. Crisci, A.; Baillet, F.; Mermoux, M.; Bogdan, G.; Nesladek, M.; Haenen, K. Residual strain around grown-in defects in CVD diamond single crystals: A 2D and 3D Raman imaging study. *Phys. Status Solidi A* **2011**, *208*, 2038–2044. [CrossRef]
12. Nasdala, L.; Hofmeister, W.; Harris, J.W.; Glinnemann, J. Growth zoning and strain patterns inside diamond crystals as revealed by Raman maps. *Am. Mineral.* **2005**, *90*, 745–748. [CrossRef]
13. Ohmagari, S.; Yamada, H.; Umezawa, H.; Chayahara, A.; Teraji, T.; Shikata, S. Characterization of free-standing single-crystal diamond prepared by hot-filament chemical vapor deposition. *Diam. Relat. Mater.* **2014**, *48*, 19–23. [CrossRef]
14. Shimizu, R.; Ogasawara, Y. Radiation damage to Kokchetav UHPM diamonds in zircon: Variations in Raman, photoluminescence, and cathodoluminescence spectra. *Lithos* **2014**, *206*, 201–213. [CrossRef]
15. Deslandes, A.; Guenette, M.C.; Belay, K.; Elliman, R.G.; Karatchevtseva, I.; Thomsen, L.; Riley, D.P.; Lumpkin, G.R. Diamond structure recovery during ion irradiation at elevated temperatures. *Nucl. Instrum. Methods Phys. Res. B* **2015**, *365*, 331–335. [CrossRef]
16. Li, Y.; Zhou, Z.X.; Guan, X.M.; Li, S.S.; Wang, Y.; Jia, X.P.; Ma, H.A. B–C bond in diamond single crystal synthesized with h-BN additive at high pressure and high temperature. *Chin. Phys. Lett.* **2016**, *33*, 028101.
17. Eaton-Magana, S.C.; Moe, K.S. Temperature effects on radiation stains in natural diamonds. *Diam. Relat. Mater.* **2016**, *64*, 130–142. [CrossRef]
18. Nasdala, L.; Steger, S.; Reissner, C. Raman study of diamond-based abrasives, and possible artefacts in detecting UHP microdiamond. *Lithos* **2016**, *265*, 317–327. [CrossRef]
19. Bensalah, H.; Stenger, I.; Sakr, G.; Barjon, J.; Bachelet, R.; Tallaire, A.; Achard, J.; Vaissiere, N.; Lee, K.H.; Saada, S.; et al. Mosaicity, dislocations and strain in heteroepitaxial diamond grown on iridium. *Diam. Relat. Mater.* **2016**, *66*, 188–195. [CrossRef]
20. Tang, Y.H.; Golding, B. Stress engineering of high-quality single crystal diamond by heteroepitaxial lateral overgrowth. *Appl. Phys. Lett.* **2016**, *108*, 052101. [CrossRef]
21. Surovtsev, N.V.; Kupriyanov, I.N. Temperature dependence of the Raman line width in diamond: Revisited. *J. Raman Spectrosc.* **2015**, *46*, 171–176. [CrossRef]
22. Hanzawa, H.; Umemura, N.; Nisida, Y.; Kanda, H.; Okada, M.; Kobayashi, M. Disorder effects of nitrogen impurities, irradiation-induced defects, and $^{13}C$ isotope composition on the Raman spectrum in synthetic Ib diamond. *Phys. Rev. B* **1996**, *54*, 3793–3799. [CrossRef]
23. Surovtsev, N.V.; Kupriyanov, I.N.; Malinovsky, V.K.; Gusev, V.A.; Pal'yanov, Y.N. Effect of nitrogen impurities on the Raman line width in diamonds. *J. Phys Condens. Matter* **1999**, *11*, 4767–4774. [CrossRef]
24. Lucazeau, G. Effect of pressure and temperature on Raman spectra of solids: Anharmonicity. *J. Raman Spectrosc.* **2003**, *34*, 478–496. [CrossRef]
25. Kolesov, B.A. How the vibrational frequency varies with temperature. *J. Raman Spectrosc.* **2017**, *48*, 323–326. [CrossRef]
26. Balkanski, M.; Wallis, R.F.; Haro, E. Anharmonic effects in light scattering due to optical phonons in silicon. *Phys. Rev. B* **1983**, *28*, 1928–1934. [CrossRef]
27. Briddon, P.R.; Jones, R. Theory of impurities in diamond. *Physica B* **1993**, *185*, 179–189. [CrossRef]
28. Ager, J.W., III; Veirs, D.K.; Rosenblatt, G.M. Spatially resolved Raman studies of diamond films grown by chemical vapor deposition. *Phys. Rev. B* **1991**, *43*, 6491. [CrossRef]
29. Kitajima, M. Defects in crystals studied by Raman scattering. *Crit. Rev. Solid State Mater. Sci.* **1997**, *22*, 275–349. [CrossRef]
30. Richter, H.; Wang, Z.P.; Ley, L. The one phonon Raman spectrum in microcrystalline silicon. *Solid State Commun.* **1981**, *39*, 625–629. [CrossRef]
31. Falkovsky, L.A. Width of optical phonons: Influence of defects of various geometry. *Phys. Rev. B* **2001**, *64*, 024301. [CrossRef]
32. Lang, A.R.; Moore, M.; Makepeace, A.P.W.; Wierzchowski, W.; Welbourn, C.M. On the dilatation of synthetic type Ib diamond by substitutional nitrogen impurity. *Philos. Trans. R. Soc. Lond. A* **1991**, *337*, 497–520. [CrossRef]

33. Grimsditch, M.H.; Anastassakis, E.; Cardona, M. Effect of uniaxial stress on the one-center optical phonon of diamond. *Phys. Rev. B* **1978**, *18*, 901–904. [CrossRef]
34. Palyanov, Y.N.; Borzdov, Y.M.; Khokhryakov, A.F.; Kupriyanov, I.N.; Sokol, A.G. Effect of nitrogen impurity on diamond crystal growth processes. *Cryst. Growth Des.* **2010**, *10*, 3169–3175. [CrossRef]
35. Zaitsev, A.M. *Handbook of Industrial Diamonds and Diamond Films*; Prelas, M., Popovici, G., Bigelow, L., Eds.; Marcel Dekker Inc.: New York, NY, USA, 1997; pp. 227–376.